6.3

DAILY TEMPERATURE AND PRECIPITATION MAPS WITH 1 KM RESOLUTION DERIVED FROM NORWEGIAN WEATHER OBSERVATIONS

M. Mohr and O. E. Tveito*
Norwegian Meteorological Institute, Oslo, Norway

1. INTRODUCTION

Daily maps of temperature and precipitation with 1 km horizontal resolution for the whole of Norway are produced for seNorge.no from daily observations of 24-hour mean temperature and 24-hour accumulated precipitation. The seNorge website is run and maintained by the Norwegian Water and Energy Directorate (NVE), the Norwegian Meteorological Institute (met.no) and the Norwegian Mapping Authorities. The website is useful for hazard mitigation, especially in conjunction with floods, droughts, energy supply shortages, avalanches and landslides.

Spatial interpolation of temperature and precipitation observations was previously done in ArcInfo (e.g. Jansson et al., 2007). However, since ArcInfo is not an operational platform at met.no, new routines had to be developed. The new routines are much faster to run and more flexible than the ArcInfo scripts that were used until now (Mohr, 2008).

Daily temperature and precipitation maps were produced for the last 3 ½ years and a cross validation of the results was carried out. For temperature about 180 stations are available in the cross validation, whereas for precipitation about 400 stations are available. Most of the stations, however, are situated at the coast or in mountain valleys, with only a few stations situated at higher elevations.

2. TEMPERATURE MAPS

2.1 Gridding of Temperature Observations

The number of stations with daily 24-hour mean temperature records varies between 150 and 200.

Measured 24-hour mean temperatures are first "de-trended" using five independent variables. These are thought to describe the large-scale spatial climate trends (Tveito and Førland 1999). The de-trending method is based on the principle that temperature can be described as a sum of deterministic and stochastic processes (Tveito et al. 2000).

The five independent variables are station height, station latitude and longitude. Furthermore, the average and the lowest altitude in a circle of 20 km radius surrounding each station are used in order to determine whether a particular station is situated in a valley or on a mountain top (Tveito et al., 2000). Longitude (≈ distance to the Atlantic ocean) is thought to describe the continentality of the climate. All five dependencies are treated as linear expressions.

For the spatial interpolation of daily "de-trended" temperatures, Kriging is used in conjunction with a fixed semi-variogram, depending only upon the month when the data was measured. The semi-variograms are based upon monthly mean temperature data from the same 1152 stations in Norway, Denmark, Sweden and Finland (Tveito et al., 2000).

The method is called residual kriging or de-trended kriging. It has proven to be robust and reliable

2.2 De-Trending of Temperatures ("The De-Trending Equation")

De-trended temperatures are calculated from observed station temperatures as:

$$T_{dt} = T_{st} - v_1 \cdot z_{st} - v_2 \cdot z_m - v_3 \cdot z_n - v_4 \cdot \varphi_{st} - v_5 \cdot \lambda_{st} - c$$

where T_{st} is the measured 24-hour mean temperature at the station and T_{dt} is the de-trended 24-hour mean temperature at the same station. Moreover, z_{st} is the altitude of the station, z_m the mean altitude within a circle of 40km diameter surrounding the station, z_n the lowest altitude within a circle of 40km diameter surrounding the station, φ_{st} the latitude of the station, and λ_{st} the longitude of the station.

The stepwise linear regression coefficients v_1 to v_5 as well as the constant (c) were obtained from trend analysis, using long-term average monthly mean

* *Corresponding author address:* Matthias Mohr, Norwegian Meteorological Institute, Climatology Dept., PO Box 43, Blindern, 0313 Oslo, Norway; e-mail: matthias.mohr@met.no.

temperatures from 1152 stations in Norway, Denmark, Sweden and Finland (Tveito et al. 2000). The monthly values for these coefficients (Table 1) are used for the daily de-trending as well.

Table 1. Monthly stepwise linear regression coefficients and constants used for calculating de-trended 24-hour mean temperatures. Regression coefficients and constants are chosen depending only upon the month of the observations. Only 4 of the 12 months are shown here.

Month	Jan	Apr	Jul	Oct
v_1 (coefficient for z_{st})	-0.0012	-0.0061	-0.0061	-0.0046
v_2 (coefficient for z_m)	-0.0051	-0.0006	0.0009	-0.0016
v_3 (coefficient for z_n)	-0.0083	-0.0008	0.0016	-0.0017
v_4 (coefficient for φ_{st})	-0.2694	-0.3288	-0.3700	-0.3349
v_5 (coefficient for λ_{st})	-0.4395	-0.1505	0.1290	-0.1581
c (constant)	19.4879	26.0346	35.9240	29.1849

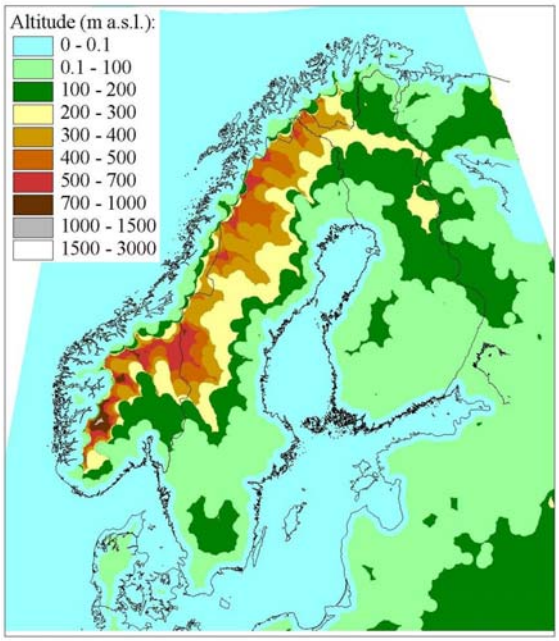

Figure 1. Spatial variation of z_n (= the lowest altitude within a circle of 40km diameter).

The de-trended 24-hour mean temperatures from all available stations (T_{dt} in equation above) were finally interpolated to the whole of Norway.

2.3 Interpolation of De-Trended Temperatures

Spatial interpolation of de-trended temperatures is done using ordinary two-dimensional kriging. The GSLIB routine "okb2d.f90" (Deutsch and Journel, 1992) is used. (Previously in ArcInfo, the Topogrid function was used, which is based upon the ANUDEM pacakage of Hutchinson (1989).)

Semi-variograms were selected depending only upon the month when the data was measured. The monthly semi-variograms from Tveito et al. (2000) were used (Table 2). The same 1152 stations from Denmark, Norway, Sweden and Finland were used to estimate these semi-variograms as were used to compute the linear regression coefficients in the de-trending equation (Tveito et al. 2000).

Table 2. Semi-variogram parameters used in the Kriging of daily de-trended temperatures. The semi-variograms were established from long-term average monthly mean temperature data (see text). Nugget values were set to zero in the study presented herein.

Month	Nugget	Sill	Range (km)
Jan	0.0	7.0	250 *
Feb	0.0	5.0	250 *
Mar	0.0	1.3	200 *
Apr	0.0	0.33	100 *
May	0.0	0.7	75 *
Jun	0.0	1.0	150 *
Jul	0.0	0.6	500**
Aug	0.0	0.19	100 *
Sep	0.0	0.3	75 *
Oct	0.0	1.3	175 *
Nov	0.0	3.5	200 *
Dec	0.0	7.0	250 *

*) Exponential model applied **) Spherical model applied

2.4 Calculation of Final Temperature Maps

Interpolated de-trended temperatures were used to produce a temperature map with 1 x 1 km horizontal resolution for the whole of Norway. For this purpose, the de-trending equation is used replacing station-related quantities with grid-point dependent quantities.

Hence, daily temperature maps are calculated as:

$$T_m(i,j) = T_{dt}(i,j) + v_1 \cdot z_{DEM}(i,j) + v_2 \cdot z_m(i,j) + v_3 \cdot z_n(i,j) + v_4 \cdot \varphi(i,j) + v_5 \cdot \lambda(i,j) + c$$

where $T_{dt}(i, j)$ are the daily interpolated de-trended station temperatures on a 1 x 1 km grid from Ordinary Kriging. $T_m(i, j)$ are the final values of daily mean temperature on a 1 x 1 km grid that are published on seNorge. Moreover, z_{DEM} is a digital elevation model of Norway with 1 km horizontal resolution, z_m are the mean altitudes within a circle of 40km diameter surrounding each 1 x 1 km grid cell, and z_n are the lowest altitudes within a circle of 40km diameter surrounding each 1 x 1 km grid cell. Finally, φ and λ are the latitudes and longitudes of the grid cells, respectively.

An example of a seNorge daily temperature map is shown in Fig. 2. In the western parts of Norway the influence of z_n on the gridded temperature maps can clearly be seen.

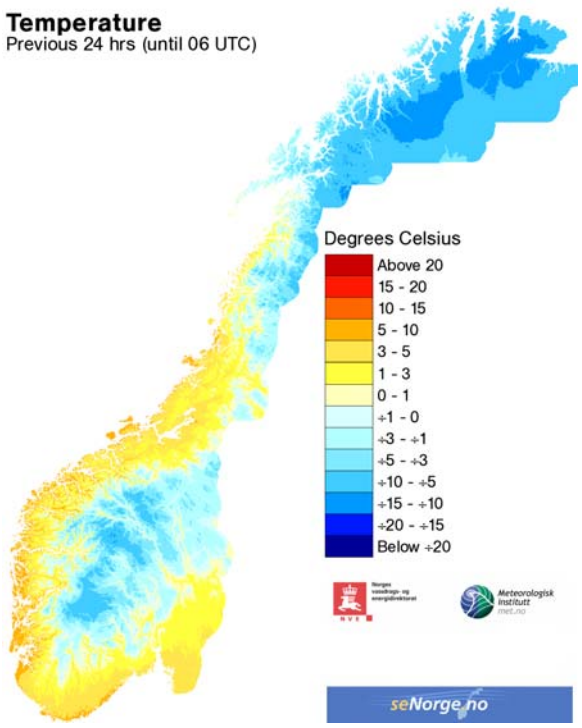

Figure 2. Daily temperature map from 30 March 2008.

3. PRECIPITATION MAPS

The Norwegian climate is characterised by extremely large variations in precipitation, mostly owing to complex topography. Mean annual precipitation can vary between 300 and more than 3000 mm over a distance of a few tens of kilometres only. In general, precipitation increases with height above sea level.

Furthermore, precipitation decreases from the western to the eastern parts of the country, due to a combination of the topography of Norway and the prevailing westerly winds.

In this study, the only factor that is taken into account is the increase of precipitation with height. It is planned, however, to include wind-direction dependent lee effects in the statistical model in the future.

3.1 Gridding of Precipitation Observations

For the spatial interpolation of precipitation, the method of triangulation is used. Gridded precipitation values are corrected for the altitude of the respective seNorge grid point, using a vertical precipitation gradient of 10% per 100 m height difference below an altitude of 1000 m above sea level as well as a gradient of 5% per 100 m height difference above an altitude of 1000 m above sea level (Mohr, 2008).

3.2 "Exposure Correction"

Observed daily 24-hour accumulated precipitation observations from all stations are corrected for measurement losses due to mainly aerodynamic effects near the rim of the gauges and blowing/drifting snow as well as for measurement losses due to evaporation and wetting (Førland et al., 1996). A distinction between liquid and solid precipitation is made.

The losses in precipitation amount can be particularly large during snowfall and high wind speeds. Even though the model from Førland et al. (1996) is recommended for monthly values only, it was used for the production of daily precipitation maps.

In this model, every station is assigned an exposure class (Table 3). Roughly, 10% of all Norwegian weather stations have been assigned an exposure class of "1", 10% an exposure class of "2", 30% an exposure class of "3", 30% an exposure class of "4" and 20% an exposure class of "5". Very exposed stations can be found at the West coast of Norway and at mountain locations. Extremely sheltered stations can be found mostly around Oslo, whereas all intermediate values can be found in between.

Table 6. Exposure correction factors used for production of daily precipitation maps. Observed precipitation is multiplied with respective correction factor. "Standard correction factors for monthly precipitation" from Førland et al. (1996) were used for correcting daily precipitation observations.

Class	Exposure	Correction factor k	
		Liquid	Solid
1	Extremely sheltered small glade in forest	1.02	1.05
2	Intermediate position between forest and plain	1.05	1.10
3	Relatively unsheltered location on a plain	1.08	1.20
4	Relatively unsheltered location in coastal or mountain region	1.11	1.40
5	Extremely unsheltered location in coastal or mountain region	1.14	1.80

Measured precipitation values are multiplied with the correction factors from Table 3. "Liquid" correction factors are applied for daily mean temperatures ≥2°C, whereas solid correction factors for daily mean temperatures <0°C. In between, an average value is used.

3.3 Triangulation of Precipitation Observations

Interpolation of "exposure corrected" precipitation observations is done by means of triangulation. Triangulation was chosen, in order to minimise the

effects of smoothing that a different interpolation method could introduce.

In our case, triangulation of precipitation involves the solution of large meshes of triangles, with hundreds of observations. The GEOMPACK Fortran 77 package was used. One disadvantage of triangulation, however, is that it is limited to cover the area between observation points. Areas outside defined triangles will be cut off.

3.4 Triangulation of Station Altitudes

In the same way as described above, station altitudes are triangulated. Hence, station altitudes above sea level are used in place of observed 24-hour accumulated precipitation values. It has to be pointed out that exactly the same triangles are used. The resulting field of triangulated station heights shall hereinafter be called $z_{st,triangulated}(i, j)$.

3.5 Calculation of Precipitation Maps

Triangulated exposure-corrected precipitation values are used in conjunction with triangulated station altitudes to produce daily precipitation maps with 1 km horizontal resolution for the whole of Norway.

Precipitation is expected to increase by about 10% per each 100 m increase in altitude. However, above 1000 m height above sea level, precipitation increases less rapidly with height. Therefore, an increase of 5% for each 100 m increase in altitude is used above this altitude. The difference between the real terrain and the triangulated station altitudes ($z_{DEM}(i, j)$ and $z_{st,triangulated}(i, j)$) is used to parameterise this increase in precipitation.

This leads to the following equations:

a) If $z_{st,triangulated}(i, j)$ < 1000 m and $z_{DEM}(i, j)$ < 1000 m:

$$rr(i,j) = rr_{st,triangulated}(i,j) \cdot \left\{1 + \frac{(z_{DEM}(i,j) - z_{st,triangulated}(i,j))}{1000}\right\}$$

b) If $z_{st,triangulated}(i, j)$ < 1000 m and $z_{DEM}(i, j)$ > 1000 m:

$$rr(i,j) = rr_{st,triangulated}(i,j) \cdot \left\{1 + \frac{(1000 - z_{st,triangulated}(i,j))}{1000} + \frac{(z_{DEM}(i,j) - 1000)}{2000}\right\}$$

c) If $z_{st,triangulated}(i, j)$ > 1000 m and $z_{DEM}(i, j)$ > 1000 m:

$$rr(i,j) = rr_{st,triangulated}(i,j) \cdot \left\{1 + \frac{(z_{DEM}(i,j) - z_{st,triangulated}(i,j))}{2000}\right\}$$

d) If $z_{st,triangulated}(i, j)$ > 1000 m and $z_{DEM}(i, j)$ < 1000 m:

$$rr\ (i,j) = rr_{st,triangulated}(i,j) \cdot \left\{1 - \frac{(z_{st,triangulated}(i,j) - 1000)}{2000} - \frac{(1000 - z_{DEM}(i,j))}{1000}\right\}$$

where $rr(i, j)$ are the final gridded values of daily precipitation that are published on seNorge.no.

An example of a daily precipitation map is shown in Fig. 3. The influence of the triangles on the gridded precipitation maps can clearly be seen.

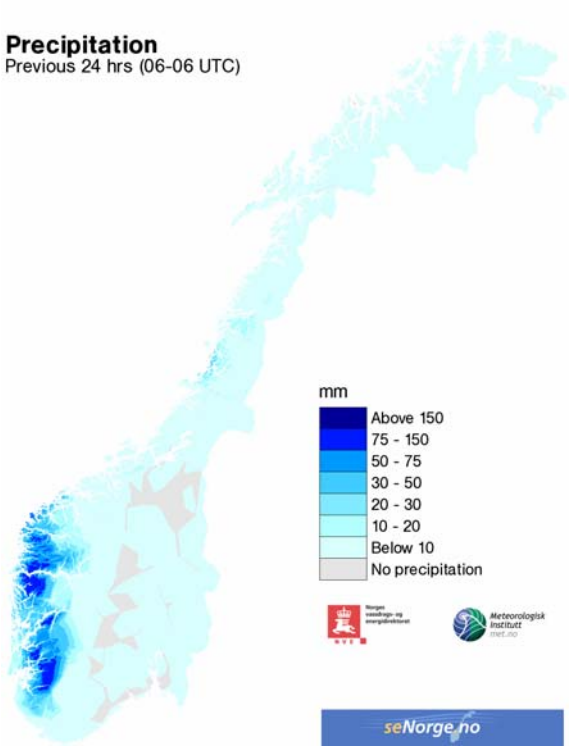

Figure 3. Daily precipitation map from 21 June 2008.

4. CROSS VALIDATION

4.1 Cross Validation of Temperature Maps

Temperature maps from 3 ½ years were cross validated using all available 24-hour mean temperature observations as input. For simplicity, de-trended temperatures were used in the cross validation presented herein instead of "real" temperatures.

Hence, de-trended temperature values were calculated at every station as described in section 2.3. All available temperature observations were used as input data except for the de-trended temperature at the station itself. This was repeated for every single day until an estimated 24-hour mean de-trended temperature and a measured 24-hour mean de-trended temperature was available at every station.

The result of the cross validation for the whole period (1 January 2005 – 26 June 2008) is shown in Fig. 4. The agreement is fairly good, with a correlation coefficient of r = 0.95. The best linear fit

has a slope of 0.90 and a y-axis intercept of 0.1 (not shown). This suggests that the simple model does not succeed totally in reproducing extreme temperature values, both on the warm side of the temperature range and on the cold side of that range.

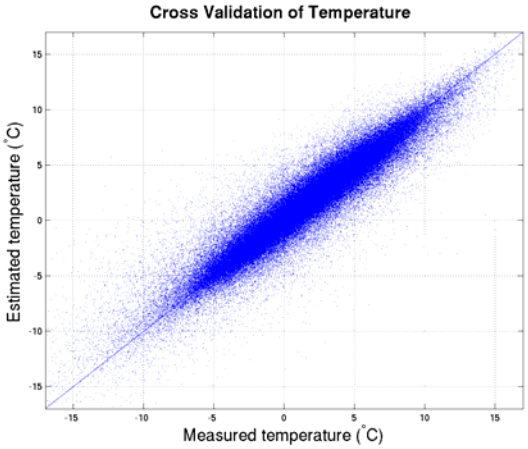

Figure 4. Cross validation of 24-hour mean temperature. Estimated temperatures from section 2.4 were compared to measured temperatures.

The mean and median values of the differences between measured and estimated 24-hour mean de-trended temperature are 0.02˚C and 0.03˚C, respectively. This suggests that there is no systematic bias. The mean absolute error of the temperature differences is 0.9˚C and the standard deviation of the error is 1.4˚C.

A histogram of the differences is shown in Fig. 5. Positive values indicate that measured temperature is greater than estimated temperature and vice versa. In general, performance is best during summer and worst during winter (Fig. 5). Indeed, for temperature July shows the best agreement and January the worst.

4.2 Cross Validation of Precipitation Maps

Precipitation maps from 3 ½ years were cross validated using all available 24-hour accumulated precipitation observations as input.

Estimated precipitation values were calculated at every station as described in section 3.5. All available precipitation observations were used as input data except for the precipitation observation at the station itself. This was repeated for every single day until an estimated 24-hour accumulated precipitation value and a measured 24-hour accumulated precipitation value was available at every station. It should be pointed out that the exposure correction from section 3.2 was not used in this comparison, as it would only disturb the analysis.

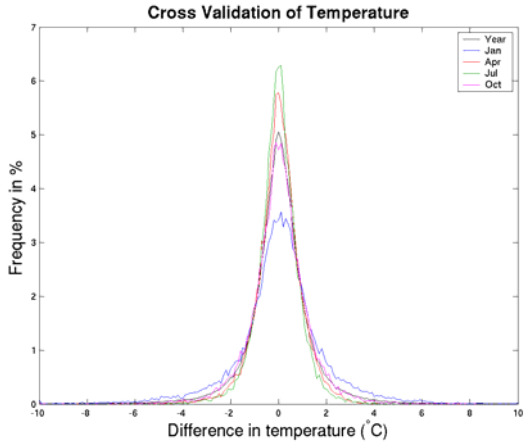

Figure 5. Same as in Fig. 4, but frequency distribution of temperature differences for the whole year as well as for the four months of January, April, July and October.

The result of the cross validation for the whole period (1 January 2005 – 26 June 2008) is shown in Fig. 6. The agreement is fairly good, with a correlation coefficient of r = 0.88. The best linear fit has a slope of 0.81 and a y-axis intercept of 0.6 (not shown). This suggests that the simple model does not succeed in reproducing extreme precipitation events, which is hardly surprising. Hence, if 100 mm of 24-hour accumulated precipitation would be observed, we could expect the model to estimate that number to 81% of the true value, i.e. to 81 mm of precipitation. However, it has to be pointed out that the scatter is huge (Fig. 6).

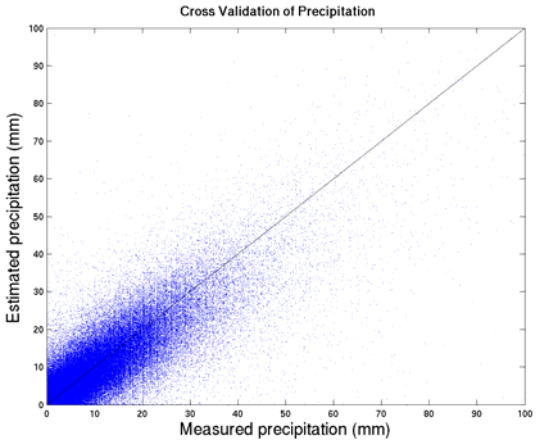

Figure 6. Cross validation of 24-hour accumulated precipitation. Estimated precipitation values from section 3.5 were compared to measured precipitation.

The mean and median values of the differences between measured and estimated 24-hour accumulated precipitation are 0.05 mm and 0.0 mm, respectively. This suggests that there is no systematic bias. The mean absolute error of the

precipitation differences is 1.5 mm and the standard deviation of the error is 3.5 mm.

A histogram of the differences between measured and estimated precipitation is shown in Fig. 7. Only cases were used where either measured or estimated precipitation is greater than 1 mm. Positive values indicate that measured precipitation is greater than estimated precipitation and vice versa.

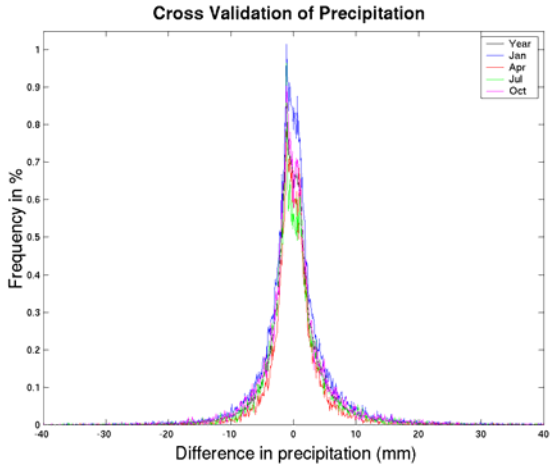

Figure 7. Same as in Fig. 6, but frequency distribution of precipitation differences for the whole year as well as for the four months of January, April, July and October. Only cases were used where either measured or estimated precipitation > 1mm.

Indeed, for precipitation January shows the best agreement and July the worst (Fig. 7). This probably reflects the higher frequency of occurence of convective precipitation events during summer.

In this case (i.e. if measured or estimated precipitation > 1 mm), the mean absolute error of the precipitation differences is 3.1 mm and the standard deviation of the error is 5.1 mm.

5. CONCLUSIONS

A fast statistical method is presented to produce spatially interpolated temperature and precipitation maps for the whole of Norway with 1 km horizontal resolution. The maps are produced operationally on a daily basis and published on the website seNorge.no. The maps are updated on a weekly basis to take temperature and precipitation observations into account that are not submitted on a daily basis or changed by the quality control system.

A cross-validation was carried out using temperature and precipitation observations from the whole of Norway for a period of 3 ½ years. For temperature, the agreement is best during summer, when there is substantial mixing within the atmospheric boundary layer and worst during winter, when inversions regularly occur.

For precipitation, the agreement is best during winter, when frontal precipitation is dominating the climate, and worst during summer, owing to frequently occurring convective precipitation events.

Correlation coefficients between estimated and measured 24-hour mean temperatures as well as 24-hour accumulated precipitation values are r = 0.95 and of r = 0.88, respectively. The slopes of the best linear fits are 0.90 and 0.81 for temperature and precipitation, respectively. This implies that extreme values of temperature and precipitation are underestimated by the statistical model with roughly 10% and 19%, respectively.

Mean absolute errors are 0.9˚C for temperature and 1.5 mm for precipitation. The standard deviations of the error are 1.4˚C for temperature and 3.5 mm for precipitation.

6. REFERENCES

Deutsch, C. V., and A. G. Journel, 1992: *GSLIB Geostatistical Software Library and User's Guide*. Oxford University Press, New York/Oxford, 340 pp.

Førland, E. J., P. Allerup, B. Dahlström, E. Elomaa, T. Jónsson, H. Madsen, J. Perälä, P. Rissanen, H. Vedin and F. Vejen, 1996: Manual for operational correction of Nordic precipitation data. *DNMI Klima Report*, 24/96 (available from met.no upon request).

Hutchinson, M. F., 1989: A new method for gridding elevation and streamline data with automatic removal of pits. *J. Hydrology*, 106, 211-232.

Jansson, A., O. E. Tveito, P. Pirinen and M. Scharling, 2007: NORDGRID – a preliminary investigation on the potential for creation of a joint Nordic gridded climate dataset. *Met.no Report*, 03/2007 (available from http://met.no/Forskning/Publikasjoner/metno_report/2007/).

Joe, B., 1991: GEOMPACK -- a software package for the generation of meshes using geometric algorithms. *Adv. Eng. Software*, 13 (5/6), 325-331.

Mohr, M., 2008: New Routines for Gridding of Temperature and Precipitation Observations for "seNorge.no". *Met.no Report*, 08/2007 (available online from http://met.no/Forskning/Publikasjoner/metno_note/2008/).

Tveito, O.E. and E.J.Førland, 1999: Mapping temperatures in Norway applying terrain information, geostatistics and GIS. *Norsk Geogr. Tidsskr.*, 53 (4), 202-212.

Tveito, O. E., E. Førland, R. Heino, I. Hansen-Bauer, H. Alexandersson, B. Dahlström, A. Drebs, C. Kern-Hansen, T. Jónsson, E. Vaarby Laursen and Y. Westman, 2000: Nordic temperature maps. *DNMI KLIMA Report*, 09/00 (available online from http://met.no/Forskning/Publikasjoner/metno_report/2000/).